energies

MDPI

Review

Research Progress on CO_2 as Geothermal Working Fluid: A Review

Lianghan Cong [1], Shuaiyi Lu [1], Pan Jiang [1], Tianqi Zheng [1], Ziwang Yu [1,*] and Xiaoshu Lü [2,3]

1 Construction Engineering College, Jilin University, Changchun 130026, China; conglh22@mails.jlu.edu.cn (L.C.)
2 Department of Electrical Engineering and Energy Technology, University of Vaasa, P.O. Box 700, FIN-65101 Vaasa, Finland
3 Department of Civil Engineering, Aalto University, P.O. Box 12100, FIN-02150 Espoo, Finland
* Correspondence: yuziw@jlu.edu.cn

Abstract: With the continuous increase in global greenhouse gas emissions, the impacts of climate change are becoming increasingly severe. In this context, geothermal energy has gained significant attention due to its numerous advantages. Alongside advancements in CO_2 geological sequestration technology, the use of CO_2 as a working fluid in geothermal systems has emerged as a key research focus. Compared to traditional water-based working fluids, CO_2 possesses lower viscosity and higher thermal expansivity, enhancing its mobility in geothermal reservoirs and enabling more efficient heat transfer. Using CO_2 as a working fluid not only improves geothermal energy extraction efficiency but also facilitates the long-term sequestration of CO_2 within reservoirs. This paper reviews recent research progress on the use of CO_2 as a working fluid in Enhanced Geothermal Systems (EGS), with a focus on its potential advantages in improving heat exchange efficiency and power generation capacity. Additionally, the study evaluates the mineralization and sequestration effects of CO_2 in reservoirs, as well as its impact on reservoir properties. Finally, the paper discusses the technological developments and economic analyses of integrating CO_2 as a working fluid with other technologies. By systematically reviewing the research on CO_2 in EGS, this study provides a theoretical foundation for the future development of geothermal energy using CO_2 as a working fluid.

Keywords: enhanced geothermal system; CO_2 as a working fluid; CO_2 storage; CO_2–enhanced geothermal system; CO_2 plume geothermal

check for updates

Citation: Cong, L.; Lu, S.; Jiang, P.; Zheng, T.; Yu, Z.; Lü, X. Research Progress on CO_2 as Geothermal Working Fluid: A Review. *Energies* **2024**, *17*, 5415. https://doi.org/10.3390/en17215415

Academic Editor: Marcin Dębowski

Received: 6 October 2024
Revised: 23 October 2024
Accepted: 25 October 2024
Published: 30 October 2024

1. Introduction

As global greenhouse gas (GHG) emissions continue to rise, hitting an all-time high in 2022, the impacts of climate change are intensifying. The world has already warmed by 1.1–1.3 °C compared to pre-industrial levels, and climate change effects are escalating. At the current pace, the remaining carbon budget for limiting warming to 1.5 °C will be exhausted in the 2020s [1]. Therefore, urgent and rapid decarbonization measures are necessary to achieve the climate goals set by the Paris Agreement. Large-scale decarbonization can be achieved through carbon dioxide removal (CDR) methods or non-CDR methods. CDR strategies focus on actively removing CO_2 from the atmosphere and safely storing it, directly addressing the rising concentration of atmospheric CO_2 and mitigating climate change. Key CDR methods include afforestation, direct air capture, and CO_2 geological sequestration. While CDR approaches hold significant potential, they are not yet ready for large-scale deployment [2].

Non-CDR strategies, such as wind, nuclear, and geothermal energy, aim to reduce emissions or improve energy efficiency, indirectly lowering atmospheric GHG concentrations [3,4]. Emissions reduction can be achieved in two ways: (1) reducing emissions from production activities or (2) controlling CO_2 emissions at the end of the process using technologies known as end-of-pipe technologies [5]. The primary contributors to global

CO_2 emissions are electricity and heat production, industry, and transportation [6,7]. These sectors' emissions can be effectively controlled by implementing methods and policies such as (1) improving energy efficiency and promoting conservation, (2) using public transportation, and (3) generating energy from renewable sources like solar or geothermal [8]. Compared to other renewable energy sources, geothermal systems offer several advantages for energy production, including (1) continuous electricity generation, (2) clean and sustainable energy production, (3) reduced CO_2 emissions and other air and water pollutants, and (4) low freshwater usage [9].

EGS involves a comprehensive system consisting of a working fluid and hot dry rock (HDR), as illustrated in Figure 1. The concept of EGS is to extract heat from "tight" rocks that have not been naturally fractured, where permeability is typically low. HDR provides the thermal energy for the system but lacks natural permeability fractures. In these cases, hydraulic fracturing or CO_2 can be used to create a heat exchange region between the HDR and the working fluid [10,11]. This process may induce seismic activity by exceeding critical fracture stress [12–14]. Geothermal power generation relies on the extraction of thermal energy, and three main technologies are employed based on working temperature: (1) flash steam, (2) dry steam, and (3) binary cycle. The first two technologies are used for high-temperature geothermal resources, while the binary cycle is used for lower temperatures [7]. Typically, water is used as the working fluid, pumped into hot rock regions where heat exchange occurs [15–17].

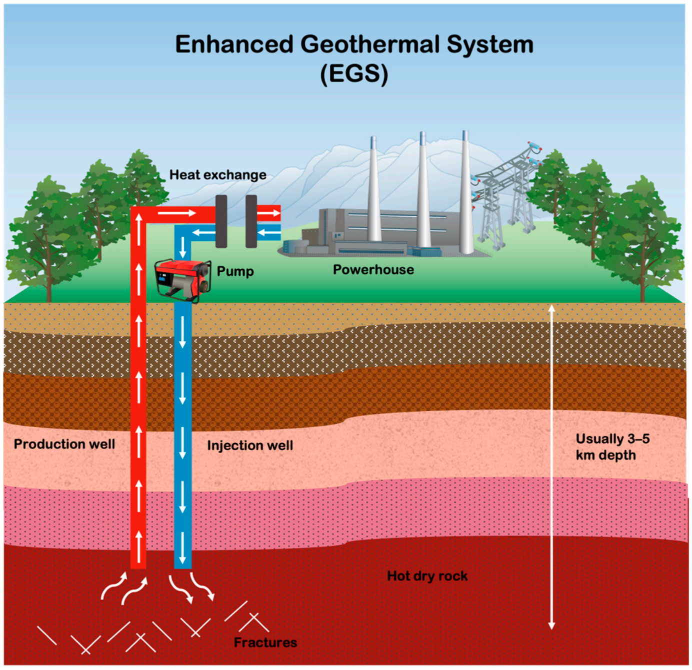

Figure 1. EGS work process.

In recent years, increasing attention has been directed toward using CO_2 as a working fluid in EGS, replacing water [5,18–21]. CO_2 offers several advantages in EGS applications: (1) CO_2 has lower viscosity, reducing energy losses during pumping and transmission in geothermal reservoirs; (2) CO_2's greater thermal expansivity results in higher efficiency, especially in lower-temperature geothermal wells, compared to traditional water-based systems; (3) CO_2 can be sequestered in subsurface reservoirs, contributing to atmospheric CO_2 reduction while also lowering water consumption; (4) CO_2 is a poor solvent for minerals, thereby reducing the risk of mineral precipitation. The use of CO_2 as a working fluid relies on advances in CO_2 geological sequestration technologies. CO_2 can be captured from industrial sources or directly from the atmosphere and stored in deep geological formations, such as depleted oil and gas reservoirs or deep saline aquifers, or even in the ocean. It is estimated that 90% of emissions from large CO_2 sources can be captured and safely stored. The use of CCS technology could reduce CO_2 emissions by 19% by 2050 [22].

In EGS, the use of CO_2 as a working fluid primarily takes two forms: CO_2-EGS and CO_2 plume geothermal (CPG) systems. Figure 2 illustrates the working process of CPG. CO_2-EGS focuses on enhancing geothermal energy extraction through artificial methods under various geological conditions while also achieving CO_2 sequestration [5,23–25]. In contrast, CPG leverages natural CO_2 reservoirs in specific regions, emphasizing efficient and environmentally low-impact geothermal energy development [26,27]. Previous research has largely focused on the technological development of CO_2 as a working fluid, with limited systematic overviews in this area. Therefore, this paper aims to review the recent progress in CO_2 research, examining the advantages and characteristics of CO_2 as a working fluid. By analyzing past and current studies, this paper assesses the feasibility of CO_2 sequestration in geothermal reservoirs. Finally, we review the economic research on using CO_2 as a working fluid in EGS.

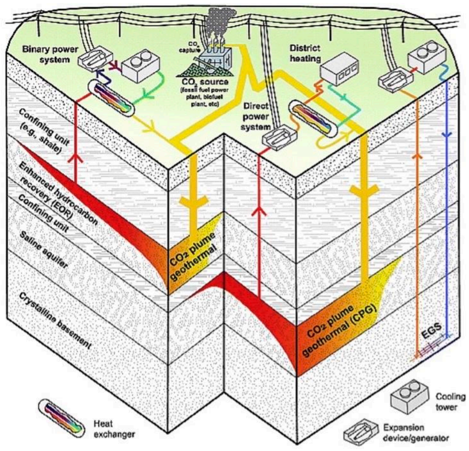

Figure 2. CPG systems [28].

2. Study of the Effect of CO_2 on Heat Transfer Efficiency

2.1. Effect of CO_2 on Heat Transfer Efficiency

CO_2 demonstrates significant differences in heat exchange efficiency compared to water. First, CO_2 has higher compressibility and expansivity, particularly at lower temperatures, which enhances its buoyancy effect during heat exchange and reduces the energy required to maintain fluid circulation. The mass flow rate of CO_2 is much higher than that of water, with an initial flow velocity approximately 3.7 times that of water, and its flow rate decreases more slowly over time. This results in a heat recovery rate that is about 50% higher for CO_2, especially in low-temperature systems, where CO_2 can extract energy more rapidly from geothermal systems. However, CO_2 has a lower specific heat capacity than water, meaning a larger mass flow is required to transfer the same amount of heat. Nevertheless, the lower viscosity of CO_2 enhances its flow capacity, making it more effective at heat transfer under a given pressure gradient compared to water. In high-temperature geothermal systems, CO_2 as a working fluid is usually under supercritical conditions. Its expansive nature allows it to absorb heat more efficiently from high-temperature heat sources. Therefore, CO_2 offers heat exchange advantages in both high- and low-temperature geothermal systems and is suitable for more efficient thermal energy recovery. Figure 3 illustrates the working process of CO_2 as a working fluid for heat exchange and power generation [21,23,29–33].

Huang et al. conducted experimental and numerical simulations to verify the heat transfer phenomena of supercritical CO_2 in geothermal reservoirs [34]. Their study identified optimal parameters for improving CO_2-EGS efficiency by setting different system pressures and mass flow rates. The results showed that CO_2 achieved the best heat transfer performance at 9 MPa and a flow rate of 0.00109 kg/s, but this seems a little unrealistic. Zhang et al. used numerical simulations to investigate the performance of CO_2-EGS and Water-EGS under different reservoir depths, temperatures, and injection pressures [35]. Even minor variations in injection temperature and pressure can have a significant impact on fluid flow within the reservoir. H_2O-EGS systems exhibit relatively stable performance, with minimal sensitivity to changes in injection parameters. However, CO_2-EGS systems are more affected by changes in injection temperature and pressure. Higher injection temperatures and lower injection pressures lead to more significant declines in system performance. Bongole et al. studied the differences in the response of injected fluids in H_2O-EGS and CO_2-EGS systems with multiple fractures [23]. The results indicated that supercritical CO_2 exhibits clear advantages in both fluid mobility and thermal conduction, leading to superior heat extraction performance in complex fracture networks compared to H_2O-EGS. In the early stage, this is primarily due to the higher flow velocity and pressure of CO_2 within the fracture network, which tends to follow high-permeability fractures, whereas heat breakthrough occurs earlier with water and its flow paths are more dispersed, resulting in lower heat recovery than CO_2. As heat transfer proceeds, heat recovery efficiency can be affected due to $scCO_2$'s high mobility.

Liao et al. conducted numerical simulations on the heat exchange efficiency of different working fluids in an EGS project located in Dikili, Turkey, using a three-dimensional anisotropic continuum damage-permeability model based on a thermo-hydro-mechanical coupling framework [36]. The results showed that CO_2 achieved higher final production temperatures and lower driving pressures for heat extraction compared to water. Another site-scale numerical simulation also demonstrated that CO_2 is more suitable as a working fluid. Zhao et al. performed numerical simulations on a CO_2-EGS in the Gonghe Basin, northwestern China [37]. Using T2WELL (version 2) software combined with the "MINC" (Multiple Interacting Continua) method, they simulated both wellbore and reservoir flows, focusing on variations in production temperature, flow rate, and heat extraction rate. Over a 30-year production period, the CO_2-EGS maintained a high heat extraction rate with lower external pumping costs.

Song et al. also conducted numerical simulations on the heat exchange efficiency of CO_2 and water. In their study, the model's geometry was subdivided using tetrahedral elements to improve simulation accuracy, and the equations were solved using tools such as Matlab and Ansys. This approach accounted for radial heat conduction, axial pressure conduction, and CO_2 compressibility, ultimately providing precise predictions of temperature and pressure distributions [38]. Compared to H_2O-EGS, the pressure drop in production wells using CO_2 was significantly smaller, only 31–45% of that for water, meaning less energy was required for fluid pumping, thus reducing energy consumption. Zhang et al. explored the heat extraction performance of supercritical CO_2 as a working fluid in EGS under different geological conditions [39]. By establishing a series of three-dimensional coupled THM models, the authors analyzed the effects of initial reservoir temperature, pressure, porosity, permeability distribution, and in situ stress conditions on the two working fluids, CO_2 and H_2O. The study found that vertical permeability anisotropy had a more significant impact on CO_2-EGS than on H_2O-EGS. Enhanced vertical permeability accelerates CO_2 flow and shortens heat exchange time. In contrast, vertical permeability anisotropy had a smaller impact on net energy output for H_2O-EGS, where production temperatures were more dependent on outlet temperature changes at the production well. Additionally, in situ stress had a greater influence on H_2O-EGS, as increased stress shortened breakthrough times, accelerating cold front penetration and resulting in greater heat losses. Table 1 shows the system conditions for heat transfer studies.

Table 1. System conditions for heat transfer studies.

Reservoir Pressure	Reservoir Temp	Velocity or Mass Flow Rate	Injection Pressure	Injection Temp	Researcher
7.5 MPa; 9 MPa; 10 MPa; 11 MPa; 12.5 MPa	200 °C	0.00082 kg/s; 0.00109 kg/s	$scCO_2$ condition	-	[34]
-	145 °C; 185 °C; 225 °C	-	8 MPa; 10 MPa	10 °C; 30 °C	[35]
-	473 K (199.85 °C)	-	17 MPa	333 K (59.85 °C)	[23]
-	170–190 °C	60 kg/s; 80 kg/s; 120 kg/s	-	-	[36]
-	353.15 K (80 °C); 398.15 K (120 °C); 458.15 K (180 °C)	-	-	308.15 K (35 °C)	[38]
35 MPa; 40 MPa; 45 MPa; 50 MPa	150 °C; 180 °C; 210 °C; 240 °C	30 L/s	-	60 °C	[39]

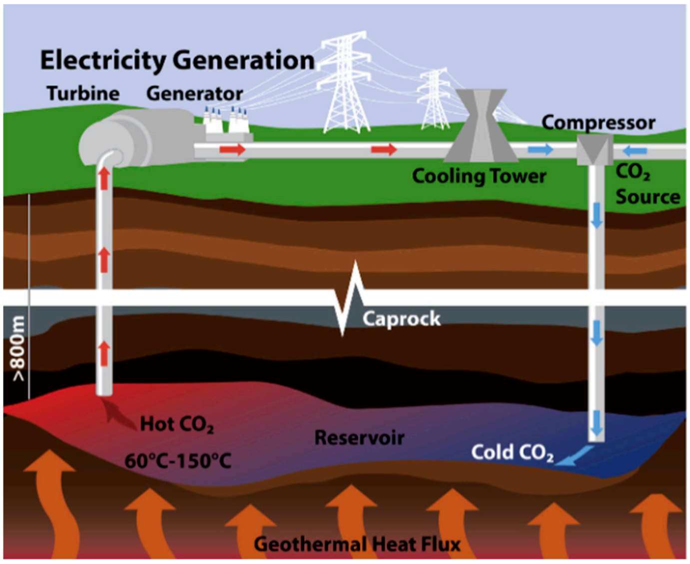

Figure 3. CO_2 as a working fluid for heat transfer and power generation [40].

2.2. *Impact of CO_2 as a Working Fluid on Power Generation*

In addition to directly affecting heat exchange efficiency, the pressure of CO_2 as a working fluid differs from that of H_2O in pipelines and equipment. In EGS, the extracted thermal energy is typically used for power generation [41], and improvements in heat exchange efficiency can have a significant impact on power generation and efficiency optimization in EGS [42–48]. Adams et al. developed four CPG models and two traditional saline geothermal systems to simulate power generation under different reservoir conditions. The model parameters included reservoir depth (1 to 5 km), geothermal gradient (20–50 °C/km), reservoir permeability (10^{-15} to 10^{-12} m^2), and wellbore diameter (0.14–0.41 m) [46]. Due to CO_2's low kinematic viscosity, it performs better in shallower, cooler, and less permeable formations, generating more electricity than saline systems. The study also confirmed that using CO_2 as a secondary fluid in Organic Rankine Cycle (ORC) systems results in higher heat transfer efficiency than the commonly used R245fa fluid.

Ezekiel et al. explored the effects of various operational parameters (such as maximum flow rate, reservoir pressure drop, and wellbore diameter) and reservoir parameters (such as permeability anisotropy and relative permeability curves) on CO_2 and water flow behavior within wells and power output [42]. Higher flow rates initially produce more electricity, as more CO_2 can be converted into electrical energy through turbines. However, excessively high flow rates cause significant pressure and temperature drops in the wellbore, increasing friction losses and leading to CO_2 vaporization or saturation pressure, which disrupts production. Simulation results indicated that to achieve circulation in the production well, the minimum apparent CO_2 velocity required is approximately 0.44–0.46 m/s for reservoir depths greater than 1500 m and 0.46–0.70 m/s for depths between 800 m and 1500 m.

Despite the advantages of using CO_2 as a working fluid, there is ongoing debate about whether it should be used exclusively. Garapati et al. compared the power generation of direct CPG hybrid systems and indirect saline geothermal systems [49]. In indirect saline systems, saline water serves as the primary heat source, transferring heat to secondary working fluids (such as CO_2) via heat exchangers before entering turbines for power generation. Both systems showed about a 20% increase in power output compared to standalone geothermal and auxiliary systems.

Fleming et al. used numerical simulations to examine the impact of water exsolution from saturated CO_2 solutions on power generation efficiency in CPG systems [15]. In geothermal reservoirs of varying depths (2.5 km to 5 km) and geothermal gradients (20 °C/km to 50 °C/km), the exsolution of water from saturated CO_2 fluids increased the fluid temperature, raising the wellhead temperature and boosting turbine output by an average of 15–25%, with a maximum increase of 41%. Qiao et al. analyzed the use of membrane-absorption separation technology to remove water from $scCO_2$-H_2O mixtures to address potential issues like water hammer and corrosion in geothermal plume systems, reducing overall system energy losses [16].

2.3. Deployment of Wells in CO_2-EGS

Shi et al. studied the efficiency of multi-branch well designs in CO_2-EGS [50]. Compared to traditional double-well CO_2-EGS, multi-branch wells exhibited superior heat extraction performance. The multi-branch design increased the contact area with the hot reservoir, improving fluid injection and production rates. Increasing the number of branches and extending well length further enhanced system performance, showing that optimizing design can prolong system life while maintaining high heat output. Although wellbore diameter had little impact on performance, proper selection of injection flow rate and production pressure was critical for stable heat extraction.

Norouzi et al. proposed using L-shaped wells for geothermal energy extraction and conducted sensitivity analyses on parameter selection in numerical simulations [51]. The analysis focused on factors such as grid resolution, well spacing optimization, channel thickness and direction, and injection rates. First, grid resolution had the greatest impact on pressure-related parameters, with coarser resolutions introducing larger errors, particularly in pressure drops. Second, well spacing optimization significantly affected CPG system performance, with adjustments improving energy extraction efficiency (CoP) and heat propagation. Channel thickness and direction also influenced heat distribution and pressure variations, with thicker channels generally enhancing system performance. Injection rates and time spans impacted optimal well spacing; larger injection ranges and rates required greater well spacing to maintain system efficiency. Appropriate well spacing maximized average power output during basin lifetime. Closer well spacing increased peak power but accelerated thermal depletion, while wider spacing preserved heat for longer but reduced flow rates, lowering power output. The study also discussed the impact of changes in injection or production well diameters on average power output, with results indicating that increasing the diameter did not necessarily lead to higher power output [46].

2.4. Carbonic Acid Corrosion of Wellbore

In geothermal systems, CO_2 corrodes mainly through its reaction with water to form carbonic acid (H_2CO_3), which triggers corrosion of pipes and cement. Carbonic acid reacts with metals, leading to localized corrosion phenomena such as metal loss and pitting, and corrosion is particularly exacerbated in high-temperature and high-pressure environments. In the case of cement, CO_2 can react with the calcium compounds in it to form calcium carbonate ($CaCO_3$), which destroys the structural integrity of the cement and leads to a loss of strength [52,53]. The acidic fluid formed by the mixing of CO_2 with water causes the pH of the cement in the wellbore to rapidly change from alkaline (~10–11) to acidic

(~4), and this pH change affects the cement–rock interface in the wellbore. Contact of the cement with CO_2 brine also triggers dissolution and precipitation, leading to redistribution of the material. These reaction products (e.g., carbonates) may migrate and re-precipitate in defective areas, thereby reducing permeability at the interface [54]. As CO_2 and brine flow through the cement–casing interface, the steel is more likely to react than the cement, generating iron carbonate deposits, which can partially fill the interface and in some instances even act as a self-seal, thus restricting further fluid flow [55]. Experimental results by Carey et al. (2010) have shown that cement is carbonated to a limited depth (50–150 µm) and does not undergo large-scale deterioration [55]. The main vulnerability of the wellbore lies in the interfacial region and not in the complete degradation of the material itself. The corrosion response of steel can be an important indicator for detecting CO_2 brine flow, and changes at the interface affect the long-term stability of the wellbore. The risk of corrosion is closely related to the concentration of CO_2, temperature, pressure, and wellbore design parameters. Corrosion may be initiated by the formation of a liquid phase, even if the water content is small. In addition, the miscibility of CO_2 with water is enhanced at high temperatures, which complicates corrosion control in the wellbore. Control of CO_2 purity can address this critical issue [56]. Connell et al. investigated the integrity and potential degradation of cement from storage wells when in contact with acidic formation water [57]. Experimental results show that most of the CO_2 leakage pathways are located at the interface between the cement and the formation or casing, rather than through the cement itself. The degree of degradation of wellbore cement is influenced by a number of factors, including the mineral composition of the cement and the concentration of calcium ions in the formation water. If the concentration of calcium ions in the formation water is high, the rate of dissolution of calcium ions slows down, thereby inhibiting further degradation of the cement. Therefore, the interaction of CO_2 with wellbore cement depends greatly on the geological environment and the properties of the cement material. Bai et al. summarized corrosion-resistant cement and steel materials in detail [58]. To resist corrosion in CO_2 injection wells, several types of cement materials are used, including modified Portland cement, calcium phosphate cement (CPC), micro-fine cement, expanding cement, and latex cement. Modified Portland cement reduces permeability by lowering the water-to-cement ratio, while CPC does not react with CO_2. Micro-fine cement fills small cracks, expanding cement enhances bonding by filling gaps, and latex cement improves elasticity and resistance to chemical attack [59–62]. Zhang et al. set experiments to test the corrosion behavior between different steel materials [63]. The temperature ranged from 50 °C to 130 °C and the pressure ranged from 80 bar to 215 bar. Lab experiments have been conducted to analyze the corrosion behavior of two low-alloyed steels (38Mn6/C75; X65), one 13Cr-steel (X20Cr13), one austenitic-ferritic steel (Duplex), CrNi-steel (1.4462), and one austenitic CrNi-steel (1.4539). The tests were conducted under supercritical CO_2 conditions in the presence of water phase. As a conclusion, the use of 13Cr-steel can be recommended.

3. CO_2 Sequestered in Underground Reservoirs by EGS

Another advantage of using CO_2 as a working fluid in geothermal systems is its ability to be sequestered in underground reservoirs [24,27,31,37,64–68]. One notable advantage of CO_2 as a working fluid is that it acts as a poor solvent for minerals, reducing the risk of mineral precipitation. However, in some saline aquifers, CO_2 reacts with brine, leading to chemical interactions with reservoir minerals that can produce stable carbonate minerals. In the study by Andrea Borgia et al. (2024), the injection of CO_2 gradually dried out the brine, inducing salt precipitation. This effect is particularly pronounced in high-salinity environments, where salt deposits can clog fractures within the reservoir, significantly reducing fluid mobility. This clogging effect compromises the efficiency of heat extraction and lowers thermal energy output [26].

Salt precipitation can occur not only within fractures but also near injection and production wells, further reducing operational efficiency and potentially shortening well lifespans. While numerical simulations suggest that under low-salinity conditions, the thermal production efficiency of CO_2 can increase by up to 360%, in high-salinity conditions, CO_2 causes a decline in reservoir permeability. The extent to which chemical reactions lead to reservoir blockage depends on the reservoir's mineralogy, brine chemistry, and CO_2 injection rate, underscoring the importance of pre-injection numerical simulations. Figure 4 depicts in detail a series of changes in a brine-containing reservoir when it comes into contact with CO_2 [69].

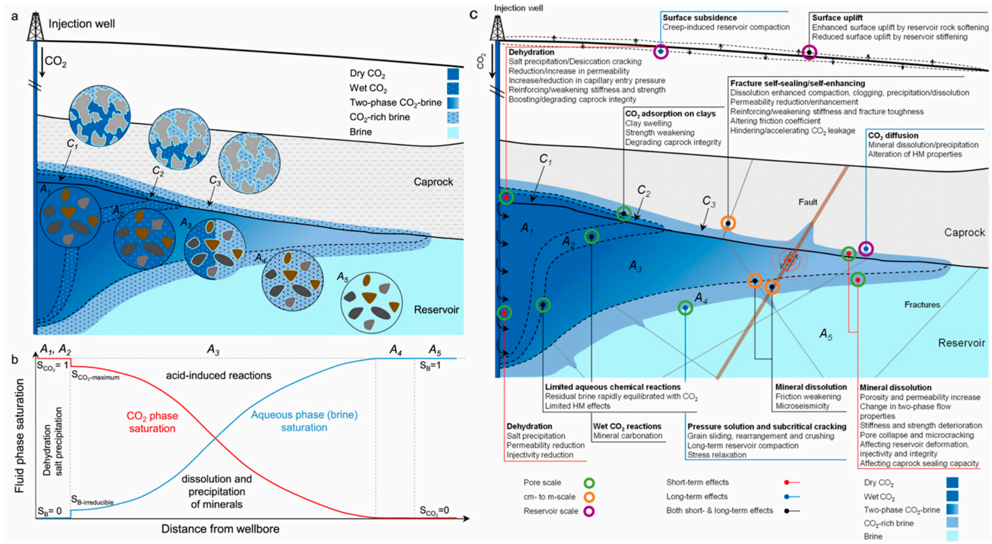

Figure 4. Schematic of a geological CO_2 storage site with zones formed around the injection well (**a**) and potential reactions in these zones (**b**). A_1 to A_4 represent zones formed in the reservoir rock. A_1, or the near-wellbore zone, is fully occupied by dry supercritical CO_2. A_3 is a two-phase flow zone and is surrounded by zones A_2 and A_4 comprising water-bearing CO_2 and CO_2-bearing brine, respectively. A_5 is the far-field or uninvaded zone. The caprock is divided into three zones: two-phase CO_2 brine zones (dry CO_2 in C_1 and wet CO_2 in C_2) and a CO_2-rich brine zone (C_3). An overview of the geochemical effects of CO_2 injection on hydromechanical properties of the reservoir and sealing rocks and the associated key issues, including reservoir injectivity, deformation and integrity, caprock integrity and sealing capacity, and induction of seismicity (**c**), from [69].

3.1. Effect of CO_2 on Reservoir Minerals

In the study by Na (2015), experimental and numerical simulation methods were used to investigate the water–rock–CO_2 reaction mechanism in the Songliao Basin's CO_2-EGS system [70]. Supercritical CO_2 promoted the dissolution of reservoir minerals, and the Ca^{2+} and Mg^{2+} ions produced combined with CO_2 in the system to form stable carbonate minerals. Due to the rapid reaction after CO_2 injection, fractures were quickly filled with CO_2, limiting further water–rock reactions, and thus the reaction rate and mineral formation were restricted. Therefore, while mineral precipitation may reduce local porosity, it does not significantly block pipelines or hinder the long-term fluid flow.

Elidemir et al. conducted a chemical analysis of CO_2–water–rock reactions in Turkish geothermal reservoirs, and geochemical modeling was performed for different reservoirs [64]. Two primary carbonate mechanisms were identified: (1) carbonate precipitation and (2) simultaneous carbonate precipitation and dissolution. In high-enthalpy geothermal fields, carbonate precipitation is the dominant mechanism, while in lower-temperature fields, carbonate precipitation and dissolution coexist. The dissolution process releases additional cations that react with CO_2. These varying mechanisms can affect the long-term properties of reservoirs, especially since carbonate precipitation reduces reservoir porosity, impacting fluid flow.

During thermal extraction, due to the viscosity differences between CO_2 and water, high-gas-saturation preferential flow channels form in the fracture network, and the CO_2

mass stored is positively correlated with the injection rate [36]. Wu et al. simulated the two-phase flow process in an EGS reservoir by alternating the injection of water and supercritical CO_2 into granite, extending the water–CO_2–rock interaction time [24]. This experimental design provided insights into CO_2 flow in rock fractures under high-temperature and high-pressure conditions, as well as mineral dissolution and precipitation processes, helping assess CO_2 storage capacity and mineralization rates. Feldspar was found to be the first mineral to dissolve, while carbonate minerals such as calcite and dolomite became the main forms of carbon storage. The concentrations of cations (such as H^+, Na^+, and Ca^{2+}) and anions (such as $CO_3{}^{2-}$ and $HCO_3{}^{-}$) in the solution were in charge balance, which could be used to estimate the amount of dissolved CO_2 [66].

Li et al. conducted similar experiments, focusing on reservoir permeability and emphasizing the importance of CO_2 injection rate [71]. The results indicated that with increased injection cycles, minerals such as montmorillonite, calcite, illite, montmorillonite-calcium silicate, and spherulite formed, promoting CO_2 mineralization storage but reducing reservoir permeability. In the absence of proppant, the permeability decreased in three stages: a rapid drop, a slow decline, another sharp drop, and then a slow decrease. When proppants were used, permeability increased by two orders of magnitude. Thus, increasing the non-contact area of the primary fractures and the flow rate of CO_2 can prevent large decreases in permeability, enhancing heat extraction and CO_2 mineralization storage.

In CPG systems, capillary backflow plays a role in returning salts to dry areas, promoting salt precipitation. As the CO_2 plume expands, backflow intensity gradually weakens, leading to salt precipitation primarily near the injection well. Salt precipitation reduces reservoir porosity and permeability, causing reservoir damage (especially near the injection well). This porosity reduction restricts fluid flow, increases system resistance, and results in greater pressure drops. When CO_2 is injected into the reservoir, the formation of dry-out zones accelerates water evaporation, further contributing to salt precipitation. Capillary pressure drives salt deposition near the wellbore, increasing bottom hole pressure (BHP) and necessitating greater pumping capacity, thereby raising operational costs. Consequently, salt precipitation both affects the long-term performance of the reservoir and increases energy and equipment demands [48].

3.2. Impact of CO_2 on Reservoir Properties

In CO_2 geological sequestration, higher reservoir permeability and lower caprock permeability favor successful storage, and CO_2 injection affects the porosity and permeability of the reservoir [14,22,72,73]. The injection of working fluids in EGS influences the mechanical state of the reservoir, leading to deformation. In H_2O-EGS systems, water provides a good medium for ion exchange, and the rapid dissolution of rock and formation of secondary minerals increases the risk of clogging transmission channels [41,68]. Using CO_2 as a working fluid largely avoids this risk but can still impact the properties of reservoir rocks.

Bongole et al. found that H_2O-EGS results in a larger reservoir deformation zone compared to CO_2-EGS [23]. Xiao et al. explored the dynamic evolution of reservoir porosity and permeability using a coupled THM model based on the Discrete Fracture Network (DFN) theory [74]. They conducted sensitivity analyses on different parameters (such as injection pressure and temperature) and found that these parameters had a significant effect on heat transfer within the reservoir. Additionally, the study validated the model by comparing numerical simulations with analytical solutions, demonstrating the model's effectiveness. The study also suggested that $scCO_2$ can effectively extract heat in EGS, supporting geothermal energy utilization and carbon emission reduction goals.

Reservoir changes are mainly driven by the combined effects of temperature, pressure, and stress fields. Once a thermal reservoir forms, the injection of $scCO_2$ causes stress field changes due to heat conduction and fluid flow, leading to thermal contraction of the rock matrix, which impacts porosity and permeability. These changes increase fluid flow rates and improve heat transfer efficiency. In low-temperature regions, the thermal contraction effect on the rock matrix is more pronounced, resulting in gradual increases in reservoir porosity and permeability. Shu et al. studied the changes in pore structure and mechanical properties of granite under different water–rock interaction conditions in the presence of $scCO_2$ [75]. The results showed that $scCO_2$ led to hydrolysis reactions in granite, forming carbonate minerals and altering the rock's pore structure and mechanical properties. Specifically, the specific surface area and pore volume of granite increased significantly, while P-wave velocity and uniaxial compressive strength decreased, especially in the presence of higher water content, where mechanical performance declined significantly.

3.3. Influence of Reservoir State on Geothermal Energy from CO_2 Extraction

The closure of a reservoir plays a significant role in the effectiveness of heat extraction and CO_2 sequestration [76]. In open-boundary reservoirs, CO_2 and heat are able to diffuse into the surrounding areas, allowing for a greater amount of CO_2 storage but resulting in less recoverable heat. On the other hand, in closed-boundary reservoirs, where CO_2 cannot diffuse due to boundary constraints, more heat can be recovered but the amount of CO_2 stored is relatively lower. From an economic perspective, while closed systems generate more revenue from electricity production, open systems yield higher overall profits due to the additional benefits of CO_2 storage. Technically, open systems require more CO_2 injection, and the reservoir lifespan tends to be longer. In contrast, closed systems focus on heat recovery, providing higher heat flux density in a shorter time frame, though the reservoir lifespan is reduced.

Geological heterogeneity significantly influences the coupled process of CO_2 storage and geothermal energy extraction in inclined reservoirs [14]. Heterogeneity causes substantial differences in reservoir porosity and permeability, leading to preferential flow pathways that result in uneven CO_2 and heat transport. In areas with high-permeability channels, CO_2 flows faster, potentially breaking through production wells early, which reduces the time available for heat recovery from the reservoir. In inclined reservoirs, CO_2 migration is notably affected by slope gradients, where steeper slopes may cause CO_2 to rise, reducing effective storage space and impacting geothermal recovery efficiency.

Injecting low-salinity water or combining CO_2 and steam injections can reduce salt precipitation and improve heat extraction efficiency. The initial temperature and pressure of the geothermal reservoir are key factors, with higher temperatures leading to higher heat extraction rates. However, excessive pressure may reduce efficiency. Reservoir porosity and permeability are also critical: high porosity and permeability support fluid flow, but high permeability can lead to early thermal breakthroughs, reducing heat extraction rates. Additionally, the phase change of CO_2 (e.g., the Joule–Thomson effect) may cause sudden temperature drops, affecting the efficiency of sustained heat extraction [43,74,77].

Yerima et al. used a combination of 3D seismic techniques, borehole analysis, and numerical modeling to assess CO_2 storage capacity in reservoirs and their energy output potential in CPG systems [65]. Reservoir porosity and permeability varied significantly across different structural stages, with the dissolution and dolomitization of carbonate rocks notably improving reservoir properties, enhancing gas storage and heat transfer capabilities. CO_2 injection increased Ca^{2+} concentrations in reservoir rocks, promoting the dissolution of calcium carbonate, which further improved reservoir permeability. The presence of caves and fractures in the reservoir aids CO_2 storage, though they also pose risks of seal failure or heat loss. In EGS, shutting down wells between injection and recovery cycles can increase CO_2 storage [66]. Although scenarios with maximum CO_2 injection may not optimize geothermal energy production efficiency, the overall heat output remains higher than the energy required for CO_2 injection and compression.

4. Economic Study of CO_2 as a Working Fluid

Economic viability and financial profitability are usually the first considerations for investors when deciding whether to invest in resource development. For geothermal energy (GE) systems, the situation is even more complex. Geothermal power plants typically require a longer payback period (about 5–7 years) and have higher initial investment costs than other renewable energy plants [78]. In addition, the size and quality of the geothermal resource often cannot be fully determined until drilling is completed. As a result, investment in geothermal technology is relatively risky [79].

The economic viability of geothermal power plants is a critical step in advancing GE systems. Since the heat flux from the earth's crust to the GE system is relatively constant, it can be used as a baseload power plant when the quality of the thermal resource is appreciable [80]. However, the profitability of low-temperature geothermal power plants is not always guaranteed due to the high drilling costs of geothermal wells [81].

For the economic assessment of geothermal power plants, several methods are commonly used. One is to calculate the costs of Enhanced Geothermal Systems, which are mainly comprised of the following aspects [41,45,82,83]:

(1) Drilling costs;
(2) Geothermal reservoir development costs;
(3) Power plant construction costs;
(4) Operation and Maintenance (O&M) costs;
(5) Heat decline rate.

Another well-established method is the levelized cost of electricity (LCOE), which is defined as the cost per unit of energy required to recover the capital investment over the entire project lifecycle. The LCOE analysis not only includes the plant's operation and maintenance costs over its lifecycle but also takes into account a number of key factors [84]:

(1) Investment costs;
(2) Average rate of power production;
(3) Lifetime;
(4) Discount rate;
(5) Availability of the facility.

In addition to research on heat exchange efficiency, current studies primarily focus on the synergistic benefits of geothermal systems with working fluids like CO_2, particularly in CO_2 sequestration [16,40,47,50,85–92].

4.1. Reduced Costs Through Lower Energy Losses

Before using CO_2 as a working fluid for geothermal energy extraction, a stable CO_2 source is required, most of which comes from capture equipment in industrial processes such as power plants and cement factories. The purity of CO_2 varies depending on the industrial process and capture method, and purifying CO_2 to remove impurities incurs additional economic costs [93]. Therefore, using CO_2 with impurities as the working fluid can significantly reduce the costs of EGS. Zhang et al. conducted a numerical simulation study on using impure CO_2 as a working fluid in EGS [85]. Impure CO_2 has a strong buoyancy effect, enabling higher self-driven flow rates and reducing the need for additional pumping energy. However, increasing the impurity content in CO_2 lowers system efficiency. This is because impure CO_2 has a lower specific heat capacity, leading to reduced heat transfer efficiency and increased irreversible losses. Additionally, higher impurity levels raise the critical pressure of the system, which increases operational pressure and, consequently, the operation and maintenance costs of the equipment. Thus, whether impure CO_2 can be used depends on specific site conditions and the potential cost savings.

In Liu's research, N_2O was used as a working fluid, showing better heat exchange performance than CO_2 and H_2O [29]. However, considering that N_2O is not easily captured and offers no synergistic benefits, this approach is not a practical option. Tagliaferri et al. conducted an economic assessment of using $scCO_2$ as a working fluid in EGS [86]. The results showed that when mass flow rates are low, $scCO_2$-EGS produces insufficient power, leading to a LCOE of up to 900 euros per megawatt-hour, which is economically unfeasible. For higher mass flow rates, the LCOE ranged between 118 and 220 euros per megawatt-hour, still relatively high under current market conditions. Furthermore,

$scCO_2$-EGS technology is not yet fully mature, with an internal rate of return (IRR) lower than the assumed discount rate and project payback periods exceeding 25 years, making short-term economic viability difficult to achieve. Although CO_2 as a working fluid shows good heat exchange efficiency in shallow geothermal areas, the method has not yet been fully commercialized.

Fleming et al. proposed the concept of a CPG-F power plant [47]. Unlike traditional CPG power plants, the CPG-F system uses two aquifers at different depths, with the shallower aquifer temporarily storing CO_2. The CPG-F system can generate power by cycling heated CO_2, while some or all of the CO_2 can be injected into the shallow aquifer for storage and released for power generation during peak demand periods. In terms of cost, the CPG-F system requires only a 3% increase in construction costs to achieve both dispatchable power generation and energy storage, and its high-efficiency flow design may result in higher initial investments. While CPG generation benefits from the synergistic effect of CO_2 sequestration, not all geological conditions can minimize the costs of both CPG power generation and CO_2 sequestration [94]. Some regions are suitable for economically efficient CO_2 storage but are not ideal for CPG power generation due to the inability to effectively extract heat from the stored CO_2.

4.2. Optimize Design or Consider Co-Benefits to Reduce Costs

Qiao et al. designed a CPG power generation system that incorporates solar energy as an auxiliary heat source and used a genetic algorithm (GA) to optimize the system's thermoeconomic performance. The optimization identified the optimal parameters, such as the main compressor inlet pressure and bypass ratio [16]. This multi-objective optimization approach improved system efficiency by 4% to 5% over conventional systems, demonstrating the potential for multi-energy synergy.

Ezekiel et al. proposed a dual-use system for CO_2, utilizing it as a working fluid to enhance natural gas recovery while extracting geothermal energy from deep gas reservoirs [95]. This system effectively reduced costs and extended the lifespan of the gas field. Simulations showed that with a CO_2 circulation rate of 110 kg/s, the system could generate a net power output of 2 MW while achieving CO_2 geological sequestration.

Chen et al. explored how CO_2 could be used as a working fluid in closed oil reservoirs for simultaneous geothermal energy extraction and CO_2 sequestration [96]. They proposed a two-stage brine extraction and CO_2 circulation strategy using two separate wells: the first stage extracts high-temperature brine from the reservoir, and the second stage extracts CO_2 through another well. This approach avoids the complexity of separating brine and CO_2 at the surface and helps mitigate reservoir pressure.

Liu et al. conducted a life cycle greenhouse gas emissions analysis for CPG systems, examining 12 scenarios that combined CPG with six CO_2 sources (e.g., BECCS, steel production) and operated in two geological settings [89]. Their study indicated that combining CPG with BECCS results in the highest greenhouse gas reduction, with life cycle emissions ranging from −0.25 to −6.18 kg CO_2 equivalent per kWh across different scenarios. Compared to other CO_2 sources (e.g., cement production, natural gas combined cycle plants, or steel mills), BECCS had higher CO_2 capture potential and lower greenhouse gas emissions.

Leveni et al. integrated technologies such as Direct Air Capture (DACC), Carbon Geological Sequestration (CGS), and EGS into the DACCUS concept [90]. DACC uses solid adsorbents or liquid solvents to capture CO_2 from the air, a process that requires low-grade thermal energy for adsorbent regeneration. Geothermal energy can supply this thermal energy and also produce electricity for DACC operations. The core of this system lies in utilizing geothermal resources in sedimentary basins, such as deep saline aquifers, combined with CO_2 geological storage to generate geothermal energy. A portion of the stored CO_2 can be circulated underground for geothermal heat extraction. This approach not only provides the necessary energy for the DACC process but also permanently stores the captured CO_2, achieving a negative emissions effect.

Liu et al. investigated the feasibility of using CO_2 as a working fluid for geothermal energy extraction and enhanced oil recovery. They employed numerical simulations to model the system and evaluate its potential, as detailed in Figure 5 [91]. Ezekiel et al. simulated subsurface wellbore fluid flow and heat transfer in a typical four-way closed anticlinal Arabian oil reservoir and optimized system power output, including a comprehensive economic analysis [82]. Their study revealed that increasing capacity factor and electricity prices had a significant positive impact on net present value (NPV), while drilling costs had the greatest negative impact on NPV for vertical wells. For horizontal wells, the levelized cost of electricity (LCOE) was lower and within a reasonable range, but for vertical wells, the LCOE was higher, leading to lower overall project profitability, with a negative NPV.

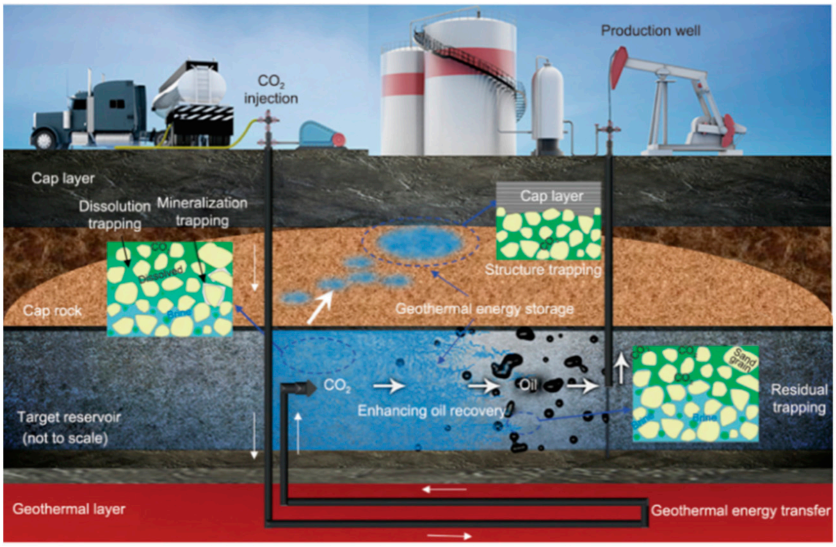

Figure 5. CO_2 as a working fluid for geothermal energy extraction with enhanced oil recovery [91].

5. Conclusions

(1) Compared to traditional water-based systems, the application of CO_2 in EGS demonstrates significant advantages. CO_2's low viscosity and high thermal expansivity allow it to circulate within geothermal reservoirs with reduced energy loss. Particularly in low-temperature geothermal conditions, the thermal expansion effect of CO_2 significantly enhances heat exchange efficiency, leading to improved heat recovery rates. Additionally, CO_2's lower viscosity enables better flow through fracture networks, reducing pumping energy consumption and extending the system's lifespan.

(2) After CO_2 is injected into the reservoir, the porosity and permeability of the reservoir are significantly affected. The flow of CO_2 not only promotes the dissolution and precipitation of minerals but also alters the mechanical properties of the reservoir. Especially under high-temperature and high-pressure conditions, CO_2 reacts quickly with minerals to form stable carbonate minerals, filling fractures and pores. Although this reaction increases the CO_2 sequestration potential to some extent, it can also reduce permeability, hindering further fluid flow. The decline in permeability generally exhibits a sharp decrease followed by gradual stabilization, but careful control of the injection rate and reservoir design can mitigate this effect.

(3) The porosity, permeability, mineral composition, and initial temperature–pressure conditions of the reservoir directly influence the heat exchange efficiency of CO_2. High porosity and moderate permeability enhance CO_2 flow and heat transfer efficiency, while geological heterogeneity and mineral reactions in the reservoir may cause thermal breakthroughs or precipitation blockages, reducing system performance. Whether the reservoir remains open also affects CO_2 heat exchange. Open-boundary reservoirs allow CO_2 and heat to diffuse into surrounding areas, resulting in greater

CO_2 storage but less recoverable heat. In contrast, closed-boundary reservoirs limit CO_2 diffusion, enabling more heat recovery but less CO_2 storage. Economically, while closed systems generate more revenue from electricity, open systems offer higher overall profits due to the additional benefits from CO_2 storage.

(4) Despite the considerable potential of CO_2 as a working fluid in improving geothermal energy extraction efficiency and achieving carbon sequestration, its commercialization still faces significant economic challenges. The costs associated with CO_2 capture, injection, and reservoir development are high, particularly for deep well drilling and system maintenance, which often exceed initial expectations. Nevertheless, through multi-objective optimization and design improvements, such as combining other renewable energy sources (e.g., solar or wind) as auxiliary heat sources, the system's thermoeconomic performance can be enhanced. Future research could focus on the CO_2 capture phase, where utilizing impure CO_2 to increase overall efficiency could significantly reduce system costs.

Author Contributions: Writing and original draft: L.C.; Investigation: S.L., P.J. and T.Z.; Review and editing: Z.Y. and X.L. All authors have read and agreed to the published version of the manuscript.

Funding: This research was funded by the National Natural Science Foundation of China (NSFC) [grant numbers 42141013, 42172274]; the cooperative project of Nanjing Center, China Geological Survey (Number: 202103); and the Scientific Research Project of Education Department of Jilin Province (JJKH20241289KJ).

Data Availability Statement: Data availability is not applicable to this article as no new data were created or analyzed in this study.

Acknowledgments: Thanks to the reviewers for their professional advice and the editors for their patience.

Conflicts of Interest: The authors declare no conflict of interest.

References

1. Lamboll, R.D.; Nicholls, Z.R.J.; Smith, C.J.; Kikstra, J.S.; Byers, E.; Rogelj, J. Assessing the Size and Uncertainty of Remaining Carbon Budgets. *Nat. Clim. Chang.* **2023**, *13*, 1360–1367. [CrossRef]
2. Ampah, J.D.; Jin, C.; Liu, H.; Afrane, S.; Adun, H.; Morrow, D.; Ho, D.T. Prioritizing Non-Carbon Dioxide Removal Mitigation Strategies Could Reduce the Negative Impacts Associated with Large-Scale Reliance on Negative Emissions. *Environ. Sci. Technol.* **2024**, *58*, 3755–3765. [CrossRef]
3. Li, Q.; Li, Q.; Wang, F.; Wu, J.; Wang, Y. The Carrying Behavior of Water-Based Fracturing Fluid in Shale Reservoir Fractures and Molecular Dynamics of Sand-Carrying Mechanism. *Processes* **2024**, *12*, 2051. [CrossRef]
4. Li, Q.; Li, Q.; Han, Y. A Numerical Investigation on Kick Control with the Displacement Kill Method during a Well Test in a Deep-Water Gas Reservoir: A Case Study. *Processes* **2024**, *12*, 2090. [CrossRef]
5. Esteves, A.F.; Santos, F.M.; Magalhães Pires, J.C. Carbon Dioxide as Geothermal Working Fluid: An Overview. *Renew. Sust. Energy Rev.* **2019**, *114*, 109331. [CrossRef]
6. Moya, M.R.; Sánchez-Cañete, E.P.; Vargas, R.; López-Ballesteros, A.; Oyonarte, C.; Kowalski, A.S.; Serrano-Ortiz, P.; Domingo, F. CO_2 Dynamics Are Strongly Influenced by Low Frequency Atmospheric Pressure Changes in Semiarid Grasslands. *J. Geophys. Res. Biogeosci.* **2019**, *124*, 902–917. [CrossRef]
7. Moya, D.; Aldás, C.; Kaparaju, P. Geothermal Energy: Power Plant Technology and Direct Heat Applications. *Renew. Sust. Energy Rev.* **2018**, *94*, 889–901. [CrossRef]
8. Yu, A.; Xing, L.; Su, W.; Liu, P. State-of-the-Art Review on the CO_2 Combined Power and Cooling System: System Configuration, Modeling and Performance. *Renew. Sust. Energ. Rev.* **2023**, *188*, 113775. [CrossRef]
9. Rohit, R.V.; Raj, R.V.; Kiplangat, D.C.; Veena, R.; Jose, R.; Pradeepkumar, A.P.; Kumar, K.S. Tracing the Evolution and Charting the Future of Geothermal Energy Research and Development. *Renew. Sust. Energ. Rev.* **2023**, *184*, 113531. [CrossRef]
10. Goodarzi, S.; Settari, A.; Zoback, M.D.; Keith, D.W. Optimization of a CO_2 Storage Project Based on Thermal, Geomechanical and Induced Fracturing Effects. *J. Pet. Sci. Eng.* **2015**, *134*, 49–59. [CrossRef]
11. Zhao, H.; Wu, K.; Huang, Z.; Xu, Z.; Shi, H.; Wang, H. Numerical Model of CO_2 Fracturing in Naturally Fractured Reservoirs. *Eng. Fract. Mech.* **2021**, *244*, 107548. [CrossRef]
12. Cappa, F.; Rutqvist, J. Impact of CO_2 Geological Sequestration on the Nucleation of Earthquakes: CO_2 CAN CAUSE EARTHQUAKES. *Geophys. Res. Lett.* **2011**, *38*. [CrossRef]

13. Perrin, C.; Manighetti, I.; Ampuero, J.-P.; Cappa, F.; Gaudemer, Y. Location of Largest Earthquake Slip and Fast Rupture Controlled by Along-Strike Change in Fault Structural Maturity Due to Fault Growth. *J. Geophys. Research. Solid Earth* **2016**, *121*. [CrossRef]
14. Cheng, Y.; Liu, W.; Xu, T.; Zhang, Y.; Zhang, X.; Xing, Y.; Feng, B.; Xia, Y. Seismicity Induced by Geological CO_2 Storage: A Review. *Earth-Sci. Rev.* **2023**, *239*, 104369. [CrossRef]
15. Fleming, M.R.; Adams, B.M.; Kuehn, T.H.; Bielicki, J.M.; Saar, M.O. Increased Power Generation Due to Exothermic Water Exsolution in CO_2 Plume Geothermal (CPG) Power Plants. *Geothermics* **2020**, *88*, 101865. [CrossRef]
16. Qiao, Z.; Cao, Y.; Li, P.; Wang, X.; Romero, C.E.; Pan, L. Thermoeconomic Analysis of a CO_2 Plume Geothermal and Supercritical CO_2 Brayton Combined Cycle Using Solar Energy as Auxiliary Heat Source. *J. Clean. Prod.* **2020**, *256*, 120374. [CrossRef]
17. Antoneas, G.; Koronaki, I. Geothermal Solutions for Urban Energy Challenges: A Focus on CO_2 Plume Geothermal Systems. *Energies* **2024**, *17*, 294. [CrossRef]
18. Sun, F.; Yao, Y.; Li, G.; Li, X. Performance of Geothermal Energy Extraction in a Horizontal Well by Using CO_2 as the Working Fluid. *Energy Conv. Manag.* **2018**, *171*, 1529–1539. [CrossRef]
19. Pan, P.; Wu, Z.; Feng, X.; Yan, F. Geomechanical Modeling of CO_2 Geological Storage: A Review. *J. Rock Mech. Geotech. Eng.* **2016**, *8*, 936–947. [CrossRef]
20. Li, H.; Wang, F.; Wang, Y.; Yuan, Y.; Feng, G.; Tian, H.; Xu, T. Phase-Field Modeling of Coupled Reactive Transport and Pore Structure Evolution Due to Mineral Dissolution in Porous Media. *J. Hydrol.* **2023**, *619*, 129363. [CrossRef]
21. Zhong, C.; Xu, T.; Gherardi, F.; Yuan, Y. Comparison of CO_2 and Water as Working Fluids for an Enhanced Geothermal System in the Gonghe Basin, Northwest China. *Gondwana Res.* **2023**, *122*, 199–214. [CrossRef]
22. Ali, M.; Jha, N.K.; Pal, N.; Keshavarz, A.; Hoteit, H.; Sarmadivaleh, M. Recent Advances in Carbon Dioxide Geological Storage, Experimental Procedures, Influencing Parameters, and Future Outlook. *Earth-Sci. Rev.* **2022**, *225*, 103895. [CrossRef]
23. Bongole, K.; Sun, Z.; Jun, Y.; Mehmood, A.; Wang, Y.; Mboje, J.; Ying, X. Multifracture Response to Supercritical CO_2-EGS and Water-EGS Based on Thermo-Hydro-Mechanical Coupling Method. *Int. J. Energy Res.* **2019**, *43*, 7173–7196. [CrossRef]
24. Wu, Y.; Li, P.; Hao, Y.; Wanniarachchi, A.; Zhang, Y.; Peng, S. Experimental Research on Carbon Storage in a CO_2-Based Enhanced Geothermal System. *Renew. Energy* **2021**, *175*, 68–79. [CrossRef]
25. Xu, R.; Zhang, L.; Zhang, F.; Jiang, P. A Review on Heat Transfer and Energy Conversion in the Enhanced Geothermal Systems with Water/CO_2 as Working Fluid. *Int. J. Energy Res.* **2015**, *39*, 1722–1741. [CrossRef]
26. Borgia, A.; Pruess, K.; Kneafsey, T.J.; Oldenburg, C.M.; Pan, L. Numerical Simulation of Salt Precipitation in the Fractures of a CO_2-Enhanced Geothermal System. *Geothermics* **2012**, *44*, 13–22. [CrossRef]
27. Singh, M.; Tangirala, S.K.; Chaudhuri, A. Potential of CO_2 Based Geothermal Energy Extraction from Hot Sedimentary and Dry Rock Reservoirs, and Enabling Carbon Geo-Sequestration. *Geomech. Geophys. Geo-Energy Geo-Resour.* **2020**, *6*, 16. [CrossRef]
28. Randolph, J.B.; Adams, B.M.; Kuehn, T.; Saar, M. Wellbore Heat Transfer in CO_2-Based Geothermal Systems. *Geotherm. Resour. Counc. Trans.* **2012**, *36*, 549–554.
29. Liu, F.; Kang, Y.; Hu, Y.; Chen, H.; Wang, X.; Pan, H.; Xie, J. Comparative Investigation on the Heat Extraction Performance of an Enhanced Geothermal System with N_2O, CO_2 and H_2O as Working Fluids. *Appl. Therm. Eng.* **2022**, *200*, 117594. [CrossRef]
30. Choi, H.S.; Park, H.C.; Huh, C.; Kang, S.-G. Numerical Simulation of Fluid Flow and Heat Transfer of Supercritical CO_2 in Micro-Porous Media. In Proceedings of the 10th International Conference on Greenhouse Gas Control Technologies, Amsterdam, The Netherlands, 19–23 September 2010; Gale, J., Hendriks, C., Turkenberg, W., Eds.; Elsevier Science Bv: Amsterdam, The Netherlands, 2011; Volume 4, pp. 3786–3793.
31. Pruess, K. Enhanced Geothermal Systems (EGS) Using CO_2 as Working Fluid—A Novel Approach for Generating Renewable Energy with Simultaneous Sequestration of Carbon. *Geothermics* **2006**, *35*, 351–367. [CrossRef]
32. Liao, Y.; Sun, X.; Sun, B.; Xu, J.; Huang, D.; Wang, Z. Coupled Thermal Model for Geothermal Exploitation via Recycling of Supercritical CO_2 in a Fracture-Wells System. *Appl. Therm. Eng.* **2019**, *159*, 113890. [CrossRef]
33. Liu, T.; Wu, P.; Chen, Z.; Li, Y. Review on Carbon Dioxide Replacement of Natural Gas Hydrate: Research Progress and Perspectives. *Energy Fuels* **2022**, *36*, 7321–7336. [CrossRef]
34. Huang, C.-J.; Hsieh, J.-C.; Lin, D.T.W.; Kuo, J.-K.; Hu, Y.-C. The Experimental Study of Heat Extraction of Supercritical CO_2 in the Geothermal Reservoir. In Proceedings of the 2016 3rd International Conference on Chemical and Biological Sciences, Amsterdam, Netherlands, 23–25 March 2016; Demetrescu, I., Oh, K., Kaushik, N.K., Butu, A., Othman, F., Eds.; EDP Sciences: Les Ulis, France, 2016; Volume 60, p. 04010.
35. Zhang, F.-Z.; Jiang, P.-X.; Xu, R.-N. System Thermodynamic Performance Comparison of CO_2-EGS and Water-EGS Systems. *Appl. Therm. Eng.* **2013**, *61*, 236–244. [CrossRef]
36. Liao, J.; Cao, C.; Hou, Z.; Mehmood, F.; Feng, W.; Yue, Y.; Liu, H. Field Scale Numerical Modeling of Heat Extraction in Geothermal Reservoir Based on Fracture Network Creation with Supercritical CO_2 as Working Fluid. *Environ. Earth Sci.* **2020**, *79*, 291. [CrossRef]
37. Zhao, W.; Yuan, Y.; Jing, T.; Zhong, C.; Wei, S.; Yin, Y.; Zhao, D.; Yuan, H.; Zheng, J.; Wang, S. Heat Production Performance from an Enhanced Geothermal System (EGS) Using CO_2 as the Working Fluid. *Energies* **2023**, *16*, 7202. [CrossRef]
38. Song, W.; Wang, C.; Du, Y.; Shen, B.; Chen, S.; Jiang, Y. Comparative Analysis on the Heat Transfer Efficiency of Supercritical CO_2 and H_2O in the Production Well of Enhanced Geothermal System. *Energy* **2020**, *205*, 118071. [CrossRef]
39. Zhang, C.; Zhang, H.; Song, R.; Wang, Z.; Jiang, G.; Zuo, Y.; Hu, J.; Huang, R. Simulation of Thermo-Hydro-Mechanical Coupled Heat Extraction Process of Geothermal Reservoir under Varied Geological Conditions with CO_2 as Working Fluid. *J. Hydrol.* **2024**, *629*, 130549. [CrossRef]

40. Bielicki, J.M.; Leveni, M.; Johnson, J.X.; Ellis, B.R. The Promise of Coupling Geologic CO_2 Storage with Sedimentary Basin Geothermal Power Generation. *iScience* **2023**, *26*, 105618. [CrossRef]
41. Olasolo, P.; Juárez, M.C.; Morales, M.P.; D'Amico, S.; Liarte, I.A. Enhanced Geothermal Systems (EGS): A Review. *Renew. Sust. Energy Rev.* **2016**, *56*, 133–144. [CrossRef]
42. Ezekiel, J.; Adams, B.M.; Saar, M.O.; Ebigbo, A. Numerical Analysis and Optimization of the Performance of CO_2-Plume Geothermal (CPG) Production Wells and Implications for Electric Power Generation. *Geothermics* **2022**, *98*, 102270. [CrossRef]
43. Garapati, N.; Randolph, J.B.; Saar, M.O. Brine Displacement by CO_2, Energy Extraction Rates, and Lifespan of a CO_2-Limited CO_2-Plume Geothermal (CPG) System with a Horizontal Production Well. *Geothermics* **2015**, *55*, 182–194. [CrossRef]
44. Qiao, Z.; Cao, Y.; Tang, Y.; Si, F. Numerical Analysis of Membrane–Absorption Separation for Supercritical Carbon Dioxide and Water Mixture of Plume Geothermal Power Generation Systems. *Energy Convers. Manag.* **2020**, *208*, 112609. [CrossRef]
45. Yerima, A.I.; Tsegab, H.; Hermana, M.; Piccoli, L.H.; Al-Masgari, A.A.-S. Feasibility of CO_2 Plume Geothermal Systems in Miocene Carbonate Reservoirs of Central Luconia Province, Offshore Sarawak: A Systematic Review of Technologies, Challenges, Mitigation Mechanisms and Economic Prospects. *J. Clean. Prod.* **2024**, *468*, 143032. [CrossRef]
46. Adams, B.M.; Vogler, D.; Kuehn, T.H.; Bielicki, J.M.; Garapati, N.; Saar, M.O. Heat Depletion in Sedimentary Basins and Its Effect on the Design and Electric Power Output of CO_2 Plume Geothermal (CPG) Systems. *Renew. Energy* **2021**, *172*, 1393–1403. [CrossRef]
47. Fleming, M.R.; Adams, B.M.; Ogland-Hand, J.D.; Bielicki, J.M.; Kuehn, T.H.; Saar, M.O. Flexible CO_2-Plume Geothermal (CPG-F): Using Geologically Stored CO_2 to Provide Dispatchable Power and Energy Storage. *Energy Convers. Manag.* **2022**, *253*, 115082. [CrossRef]
48. Norouzi, A.M.; Pouranian, F.; Rabbani, A.; Fowler, N.; Gluyas, J.; Niasar, V.; Ezekiel, J.; Babaei, M. CO_2-Plume Geothermal: Power Net Generation from 3D Fluvial Aquifers. *Appl. Energy* **2023**, *332*, 120546. [CrossRef]
49. Garapati, N.; Adams, B.M.; Fleming, M.R.; Kuehn, T.H.; Saar, M.O. Combining Brine or CO_2 Geothermal Preheating with Low-Temperature Waste Heat: A Higher-Efficiency Hybrid Geothermal Power System. *J. CO_2 Util.* **2020**, *42*, 101323. [CrossRef]
50. Shi, Y.; Song, X.; Shen, Z.; Wang, G.; Li, X.; Zheng, R.; Geng, L.; Li, J.; Zhang, S. Numerical Investigation on Heat Extraction Performance of a CO_2 Enhanced Geothermal System with Multilateral Wells. *Energy* **2018**, *163*, 38–51. [CrossRef]
51. Norouzi, A.M.; Gluyas, J.; Babaei, M. CO_2-Plume Geothermal in Fluvial Formations: A 2D Numerical Performance Study Using Subsurface Metrics and Upscaling. *Geothermics* **2022**, *99*, 102287. [CrossRef]
52. Arbad, N.; Emadi, H.; Watson, M. A Comprehensive Review of Geothermal Cementing from Well Integrity Perspective. *J. Pet. Sci. Eng.* **2022**, *217*, 110869. [CrossRef]
53. Schott, T.; Liautaud, F. Monitoring and Mitigating Corrosion in Geothermal Systems. *Mater. Corros.* **2022**, *73*, 1916–1942. [CrossRef]
54. Carey, J.W.; Svec, R.; Grigg, R.; Lichtner, P.C.; Zhang, J.; Crow, W. Wellbore Integrity and CO_2-Brine Flow along the Casing-Cement Microannulus. In Proceedings of the Greenhouse Gas Control Technologies 9, Washington DC, USA, 16–20 November 2008; Gale, J., Herzog, H., Braitsch, J., Eds.; Elsevier Science Bv: Amsterdam, The Netherlands, 2009; Volume 1, pp. 3609–3615.
55. Carey, J.W.; Svec, R.; Grigg, R.; Zhang, J.; Crow, W. Experimental Investigation of Wellbore Integrity and CO_2-Brine Flow along the Casing-Cement Microannulus. *Int. J. Greenh. Gas Control* **2010**, *4*, 272–282. [CrossRef]
56. Atrens, A.D.; Gurgenci, H.; Rudolph, V. Water Condensation in Carbon-Dioxide-Based Engineered Geothermal Power Generation. *Geothermics* **2014**, *51*, 397–405. [CrossRef]
57. Connell, L.; Down, D.; Lu, M.; Hay, D.; Heryanto, D. An Investigation into the Integrity of Wellbore Cement in CO_2 Storage Wells: Core Flooding Experiments and Simulations. *Int. J. Greenh. Gas Control* **2015**, *37*, 424–440. [CrossRef]
58. Bai, M.; Sun, J.; Song, K.; Li, L.; Qiao, Z. Well Completion and Integrity Evaluation for CO_2 Injection Wells. *Renew. Sustain. Energy Rev.* **2015**, *45*, 556–564. [CrossRef]
59. Lécolier, E.; Rivereau, A.; Ferrer, N.; Audibert, A.; Longaygue, X. Durability of Oilwell Cement Formulations Aged in H2S-Containing Fluids. *SPE Drill. Complet.* **2010**, *25*, 90–95. [CrossRef]
60. Barlet-Gouédard, V.; Rimmelé, G.; Goffé, B.; Porcherie, O. *Mitigation Strategies for the Risk of CO_2 Migration Through Wellbores*; OnePetro: Richardson, TX, USA, 2006.
61. Benge, G.; Dew, E.G. *Meeting the Challenges in Design and Execution of Two High Rate Acid Gas Injection Wells*; OnePetro: Richardson, TX, USA, 2005.
62. Fakhreldin, Y.; Al-Sharji, H.; Ruwehy, A.M.; Saadi, K.; Taoutaou, S.; Al-Kalbani, S. *Advanced Cement System for Acid Gas Injection Wells*; OnePetro: Richardson, TX, USA, 2010.
63. Zhang, Y.; Gao, K.; Schmitt, G. *Inhibition Of Steel Corrosion Under Aqueous Supercritical CO_2 Conditions*; OnePetro: Richardson, TX, USA, 2011.
64. Elidemir, S.; Gulec, N. Geochemical Characterization of Geothermal Systems in Western Anatolia (Turkey): Implications for CO_2 Trapping Mechanisms in Prospective CO_2-EGS Sites. *Greenh. Gases* **2018**, *8*, 63–76. [CrossRef]
65. Yerima, A.I.; Tsegab, H.; Hermana, M.; Piccoli, L.H. Integrated Modelling of CO_2 Plume Geothermal Energy Systems in Carbonate Reservoirs: Technology, Operations, Economics and Sustainability. *Renew. Energy* **2024**, *233*, 121162. [CrossRef]
66. Tai, N.; Gates, I.D. Cyclic CO_2 Storage and Geothermal Energy Extraction Using a Huff and Puff Technique in the Basal Cambrian Sandstone Unit, Canada. *Geothermics* **2024**, *118*, 102925. [CrossRef]

67. Yalcin, B.; Ezekiel, J.; Mai, P.M. Potential for CO_2 Plume Geothermal and CO_2 Storage in an Onshore Red Sea Rift Basin, Al-Wajj, Saudi Arabia: 3D Reservoir Modeling and Simulations. *Geothermics* **2024**, *119*, 102966. [CrossRef]
68. Li, Y.; Cui, J.; Yu, H.; Li, Y.; Tang, D.; Zhang, G.; Liu, Y. The Impacts of Geothermal Gradients on Compressed Carbon Dioxide Energy Storage in Aquifers. *Renew. Energy* **2024**, *231*, 120954. [CrossRef]
69. Vafaie, A.; Cama, J.; Soler, J.M.; Kivi, I.R.; Vilarrasa, V. Chemo-Hydro-Mechanical Effects of CO_2 Injection on Reservoir and Seal Rocks: A Review on Laboratory Experiments. *Renew. Sust. Energy Rev.* **2023**, *178*, 113270. [CrossRef]
70. Na, J.; Xu, T.; Yuan, Y.; Feng, B.; Tian, H.; Bao, X. An Integrated Study of Fluid-Rock Interaction in a CO_2-Based Enhanced Geothermal System: A Case Study of Songliao Basin, China. *Appl. Geochem.* **2015**, *59*, 166–177. [CrossRef]
71. Li, P.; Hao, Y.; Wu, Y.; Wanniarachchi, A.; Zhang, H.; Cui, Z. Experimental Study on the Effect of CO_2 Storage on the Reservoir Permeability in a CO_2-Based Enhanced Geothermal System. *Geotherm. Energy* **2023**, *11*, 24. [CrossRef]
72. Hefny, M.; Qin, C.; Saar, M.O.; Ebigbo, A. Synchrotron-Based Pore-Network Modeling of Two-Phase Flow in Nubian Sandstone and Implications for Capillary Trapping of Carbon Dioxide. *Int. J. Greenh. Gas Control.* **2020**, *103*, 103164. [CrossRef]
73. Liao, J.; Hu, K.; Mehmood, F.; Xu, B.; Teng, Y.; Wang, H.; Hou, Z.; Xie, Y. Embedded Discrete Fracture Network Method for Numerical Estimation of Long-Term Performance of CO_2-EGS under THM Coupled Framework. *Energy* **2023**, *285*, 128734. [CrossRef]
74. Xiao, X.; Li, W.; Gong, P.; Xu, J.; Ding, X. Numerical Study of Enhanced Geothermal Systems with Supercritical CO_2 Injection Considering Reservoir Changes. *Energy Sci. Eng.* **2024**, *12*, 2992–3007. [CrossRef]
75. Shu, B.; Chen, J.; Xue, H. Experimental Study of the Change of Pore Structure and Strength of Granite after Fluid-Rock Interaction in CO_2-EGS. *Renew. Energy* **2024**, *220*, 119635. [CrossRef]
76. Nematollahi, B.; Chen, M.; Nikoo, M.R.; Al-Maktoumi, A. Evaluation and Optimization of a Horizontal Well-Triplet for CO_2 Plume Geothermal Harvest: Comparison between Open and Close Reservoirs. *J. Hydrol.* **2023**, *623*, 129811. [CrossRef]
77. Cui, G.; Ren, S.; Rui, Z.; Ezekiel, J.; Zhang, L.; Wang, H. The Influence of Complicated Fluid-Rock Interactions on the Geothermal Exploitation in the CO_2 Plume Geothermal System. *Appl. Energy* **2018**, *227*, 49–63. [CrossRef]
78. Pan, S.-Y.; Gao, M.; Shah, K.J.; Zheng, J.; Pei, S.-L.; Chiang, P.-C. Establishment of Enhanced Geothermal Energy Utilization Plans: Barriers and Strategies. *Renew. Energy* **2019**, *132*, 19–32. [CrossRef]
79. Anderson, A.; Rezaie, B. Geothermal Technology: Trends and Potential Role in a Sustainable Future. *Appl. Energy* **2019**, *248*, 18–34. [CrossRef]
80. Tomasini-Montenegro, C.; Santoyo-Castelazo, E.; Gujba, H.; Romero, R.J.; Santoyo, E. Life Cycle Assessment of Geothermal Power Generation Technologies: An Updated Review. *Appl. Therm. Eng.* **2017**, *114*, 1119–1136. [CrossRef]
81. Van Erdeweghe, S.; Van Bael, J.; Laenen, B.; D'haeseleer, W. Feasibility Study of a Low-Temperature Geothermal Power Plant for Multiple Economic Scenarios. *Energy* **2018**, *155*, 1004–1012. [CrossRef]
82. Ezekiel, J.; Vahrenkamp, V.; Hoteit, H.A.; Finkbeiner, T.; Mai, P.M. Techno-Economic Assessment of Large-Scale Sedimentary Basin Stored-CO_2 Geothermal Power Generation. *Appl. Energy* **2024**, *376*, 124270. [CrossRef]
83. Pajak, L.; Sowizdzal, A.; Gladysz, P.; Tomaszewska, B.; Miecznik, M.; Andresen, T.; Frengstad, B.S.; Chmielowska, A. Multi-Criteria Studies and Assessment Supporting the Selection of Locations and Technologies Used in CO_2-EGS Systems. *Energies* **2021**, *14*, 7683. [CrossRef]
84. Soltani, M.; Moradi Kashkooli, F.; Souri, M.; Rafiei, B.; Jabarifar, M.; Gharali, K.; Nathwani, J.S. Environmental, Economic, and Social Impacts of Geothermal Energy Systems. *Renew. Sust. Energy Rev.* **2021**, *140*, 110750. [CrossRef]
85. Zhang, Y.; Yang, K.; Hong, H.; Zhong, X.; Xu, J. Thermodynamic Analysis of a Novel Energy Storage System with Carbon Dioxide as Working Fluid. *Renew. Energy* **2016**, *99*, 682–697. [CrossRef]
86. Tagliaferri, M.; Gladysz, P.; Ungar, P.; Strojny, M.; Talluri, L.; Fiaschi, D.; Manfrida, G.; Andresen, T.; Sowizdzal, A. Techno-Economic Assessment of the Supercritical Carbon Dioxide Enhanced Geothermal Systems. *Sustainability* **2022**, *14*, 16580. [CrossRef]
87. Ezekiel, J.; Kumbhat, D.; Ebigbo, A.; Adams, B.M.; Saar, M.O. Sensitivity of Reservoir and Operational Parameters on the Energy Extraction Performance of Combined CO_2-EGR-CPG Systems. *Energies* **2021**, *14*, 6122. [CrossRef]
88. McDonnell, K.; Molnar, L.; Harty, M.; Murphy, F. Feasibility Study of Carbon Dioxide Plume Geothermal Systems in Germany-Utilising Carbon Dioxide for Energy. *Energies* **2020**, *13*, 2416. [CrossRef]
89. Liu, L.; Miranda, M.M.; Bielicki, J.M.; Ellis, B.R.; Johnson, J.X. Life Cycle Greenhouse Gas Emissions of CO_2-Enabled Sedimentary Basin Geothermal. *Environ. Sci. Technol.* **2024**, *58*, 1882–1893. [CrossRef] [PubMed]
90. Leveni, M.; Bielicki, J.M. A Potential for Climate Benign Direct Air CO_2 Capture with CO_2-Driven Geothermal Utilization and Storage (DACCUS). *Environ. Res. Lett.* **2024**, *19*, 014007. [CrossRef]
91. Liu, Y.; Hu, T.; Rui, Z.; Zhang, Z.; Du, K.; Yang, T.; Dindoruk, B.; Stenby, E.H.; Torabi, F.; Afanasyev, A. An Integrated Framework for Geothermal Energy Storage with CO_2 Sequestration and Utilization. *Engineering* **2023**, *30*, 121–130. [CrossRef]
92. Rajabi, M.M.; Chen, M.; Javaran, M.R.H.; Al-Maktoumi, A.; Izady, A.; Dong, Y. Probabilistic Net Present Value Analysis for Designing Techno-Economically Optimal Sequential CO_2 Sequestration and Geothermal Energy Extraction. *J. Hydrol.* **2022**, *612*, 128237. [CrossRef]
93. Ozkan, M.; Akhavi, A.-A.; Coley, W.C.; Shang, R.; Ma, Y. Progress in Carbon Dioxide Capture Materials for Deep Decarbonization. *Chem* **2022**, *8*, 141–173. [CrossRef]

94. Ogland-Hand, J.D.; Adams, B.M.; Bennett, J.A.; Middleton, R.S. A Geospatial Cost Comparison of CO_2 Plume Geothermal (CPG) Power and Geologic CO_2 Storage. *Front. Energy Res.* **2022**, *10*. [CrossRef]
95. Ezekiel, J.; Ebigbo, A.; Adams, B.M.; Saar, M.O. Combining Natural Gas Recovery and CO_2-Based Geothermal Energy Extraction for Electric Power Generation. *Applied Energy* **2020**, *269*, 115012. [CrossRef]
96. Chen, M.; Al-Maktoumi, A.; Izady, A.; Cai, J.; Dong, Y. Use Closed Reservoirs for CO_2 Storage and Heat Recovery: A Two-Stage Brine-Extraction and CO_2-Circulation Strategy. *Sustain. Energy Technol. Assess.* **2022**, *52*, 102346. [CrossRef]